DOI: 10.1002/ejic.201000862

Photochemical Synthesis of Ruthenium–Carbonyl Compounds with Thioether Ligands and Subsequent Oxidative Cleavage of Trinuclear Complexes by Chlorinated Solvents

Biplab K. Maiti,[a] **Helmar Görls,**[a] **Olaf Klobes,**[b] **and Wolfgang Imhof***[a]

Keywords: Ruthenium / Carbonyl ligands / Thioether ligands / Photochemistry / X-ray diffraction

The photochemical reaction of [$Ru_3(CO)_{12}$] with thioether ligands in THF leads to the isolation of tetranuclear ruthenium–carbonyl cluster compounds of the formula [$Ru_4(CO)_{13}$(μ_2-R_2S)]. In these compounds, ruthenium atoms adopt a typical butterfly arrangement. If chelating ligands with two thioether functions are introduced, the reaction leads to mixtures of the trinuclear substitution products [$Ru_3(CO)_{10}$(RS∩SR)] and [$Ru_3(CO)_8$(RS∩SR)$_2$]. The latter may be oxidatively cleaved by the use of chlorinated solvents to produce the mononuclear compound [$Ru(CO)_2Cl_2$(RS∩SR)] or the dinuclear complex [$Ru_2(CO)_2$(μ_2-Cl)$_2$$Cl_2$(RS∩SR)$_2$] depending on the reaction conditions. Five new ruthenium–carbonyl–thioether complexes were characterized by X-ray diffraction.

Introduction

Quite recently, we became interested in the chemistry of thioether ligands in the coordination sphere of ruthenium due to research activities in the field of catalytic transformations of thioethers. Thioethers as well as hydrogen sulfide, thiols, and thiophenes naturally appear in fossil fuels due to the anaerobic degradation of sulfur-containing biological material such as cysteine and methionine residues in proteins.[1] They are undesirable in this respect since they tend to poison catalysts used in fuel processing as well as in exhaust gas treatment and must therefore be removed producing desulfurized fuel.[2] On the other hand, polysulfides are widely used as sealing compounds (e.g., for the production of multiply glazed windows, kerosene tanks of aircrafts, or the ground beneath gas stations). In this context, ruthenium precatalysts that already exhibit thioether ligands seem to be less prone to being poisoned by additional sulfur-containing substrates. Complexes of this type have, for example, been used for the synthesis of sulfoxides from thioethers.[3]

Thioethers in general prefer monodentate coordination modes if bound to transition metals.[4] Nevertheless, in some cases insertion reactions of metal atoms or nucleophiles in general into carbon–sulfur bonds have also been observed.[5] Moreover, compounds in which thioethers bridge two or more transition metal atoms are much less common than sulfide- or thiolate-bridged compounds. We recently published a report about the synthesis of ruthenium–carbonyl complexes with thioether ligands from the reaction of [$Ru_3(CO)_{12}$] with the respective thioethers under irradiation in chloroform.[6] Most interestingly, we observed reaction pathways in which ruthenium atoms are oxidized to the oxidation state II with chlorido ligands that originate from solvent molecules balancing the positive charge.

Herein we present results of photochemical reactions of [$Ru_3(CO)_{12}$] with the same thioether ligands under irradiation in THF. Correspondingly, no redox reaction pathways are observed. Depending on the thioether used and reaction conditions, tri- or tetranuclear ruthenium–carbonyl cluster compounds are isolated. Upon dissolving the compounds in chloroform, the former are transferred into the mononuclear Ru^{II} complexes observed before.[6]

Results and Discussion

Scheme 1 shows the reaction of [$Ru_3(CO)_{12}$] with tetrahydrothiophene (THT) and 1,4-oxathiane (OXT) in THF under irradiation with UV light. After approximately 20 min, the formation of an insoluble precipitate is observed. So the reaction time was limited to 40 min. After filtration of the precipitate and chromatographic workup, tetranuclear ruthenium cluster compounds **1a** and **1b** were isolated in low yields. Compounds **1a** and **1b** were analyzed by mass spectrometry and IR and ^{1}H NMR spectroscopy. Mass spectrosopy showed the tetranuclear composition of the compounds, and from IR spectroscopy it became evident that next to terminal CO ligands there are also bridging CO groups present. ^{1}H NMR spectra showed signals that represent methylene units at expected chemical shifts.

---

[a] Institute of Inorganic and Analytical Chemistry, Friedrich Schiller University Jena,
August-Bebel-Strasse 2, 07743 Jena, Germany
Fax: +49-3641-948102
E-mail: Wolfgang.Imhof@uni-jena.de
[b] Akzo Nobel Functional Chemicals GmbH & Co. KG,
Liebigstrasse 7, 07973 Greiz, Germany
Fax: +49-3661-78219
E-mail: Olaf.Klobes@akzonobel.com

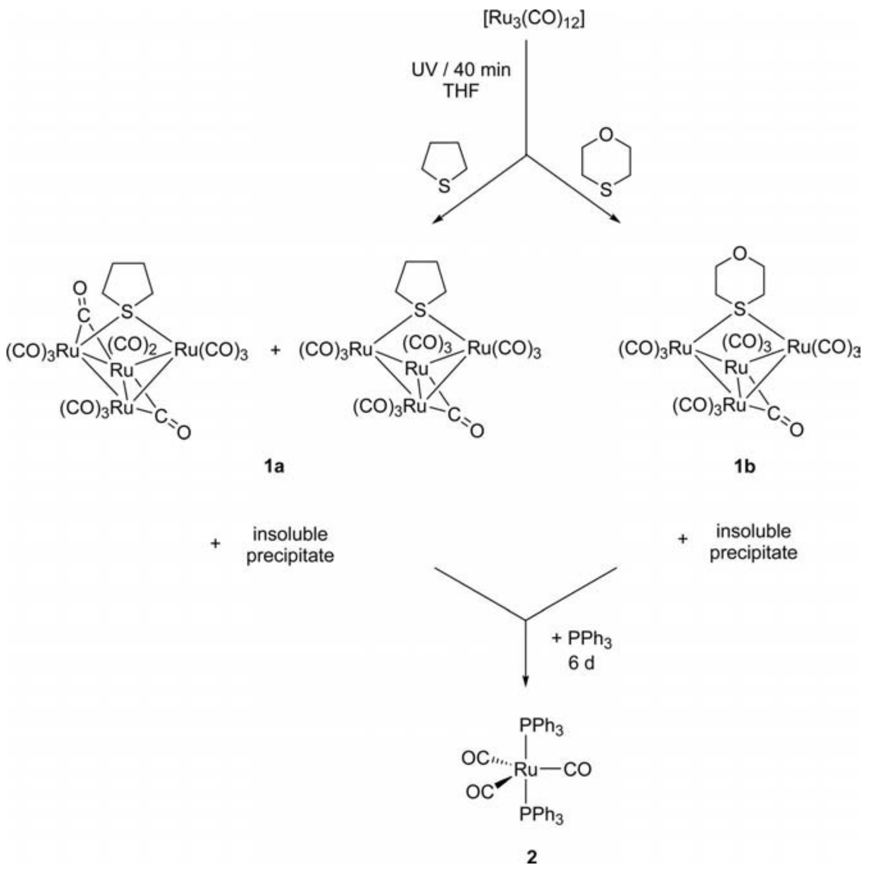

Scheme 1. Photochemical reaction of $[Ru_3(CO)_{12}]$ with heterocyclic thioethers in THF.

By recrystallization from mixtures of light petroleum and THF at 0 °C, it was possible to obtain single crystals of **1a** and **1b**. The molecular structures of two isomers of **1a** are depicted in Figure 1; Figure 2 correspondingly shows the structure of **1b**. Selected bond lengths and angles are summarized in Table 1. In the crystal structure of **1a**, two isomeric cluster compounds are observed that differ significantly with regards to the arrangement of the ruthenium centers, coordination of one CO ligand, and ruthenium–sulfur bond lengths. Nevertheless, most of the other bonding properties remain unchanged. In both compounds four ruthenium atoms are observed in a butterfly arrangement. The dihedral angle between the two Ru_3 planes are 95.3° in isomer 1 (Figure 1, top) and 84.6° in isomer 2 (Figure 1, bottom). The sulfur atoms of THT ligands bridge two of the ruthenium atoms, with the ruthenium–sulfur bonds being slightly different. In both isomers one of the CO ligands is slightly bent (isomer 1: Ru3a–C11a–O7a 159.0°; isomer 2: Ru4b–C15b–O11b 162.4°) with the corresponding carbon atom being situated quite close to another Ru atom (isomer 1: Ru2a–C11a 256.3 pm; isomer 2: Ru1b–C15b 266.2 pm). The additionally coordinated Ru2a shows the longest Ru–S bond [239.55(8) pm]. The central Ru–Ru bond of the tetranuclear cluster is bridged by another carbon monoxide ligand. However, this ligand also is not symmetrically bound, but the bond towards the ruthenium atom that is coordinated by the above-mentioned semi-bridging CO ligand is always significantly shorter than the other Ru–C bond (isomer 1: Ru3a–C14a 201.0 pm, Ru4a–C14a 231.0 pm; isomer 2: Ru3b–C14b 233.4 pm, Ru4b–C14b 201.4 pm). The molecular structure of **1b** closely resembles the situation in isomer 2 of **1a** (Figure 2, Table 1).

Only a few similar tetranuclear ruthenium compounds with bridging thioether ligands that use trithiane, 3,3-dimethylthietane, dimethyl sulfide, or even THT as ligands have been reported before.[7] These ligands are either coordinated to an $[Ru_4(CO)_{13}]$ fragment as in **1a** and **1b** or to an $[Ru_4(CO)_{12}(\mu_2\text{-}H)_2]$ fragment. There is one crystal structure of **1a** described before that is almost isostructural.[7d] Although the same structural dissimilarities between two independent molecules are also observed, they are not discussed by the authors. Moreover, their structural analysis was performed at room temperature and *R* values therefore are slightly worse than those of **1a** described herein.

According to IR spectroscopy, the precipitates that are produced during the synthesis of **1a** and **1b** are also ruthenium–carbonyl species. Although bands that correspond to the sulfur-containing ligands in **1a** and **1b** are much weaker, elemental analyses still showed that the precipitates contain sulfur. Nevertheless, hydrogen contents indicate that there should be other organic ligands in addition to THT or OXT. We therefore propose that the precipitates are polymers that exhibit thioether as well as THF ligands that at least partly bridge ruthenium atoms as in **1a** and **1b**. The

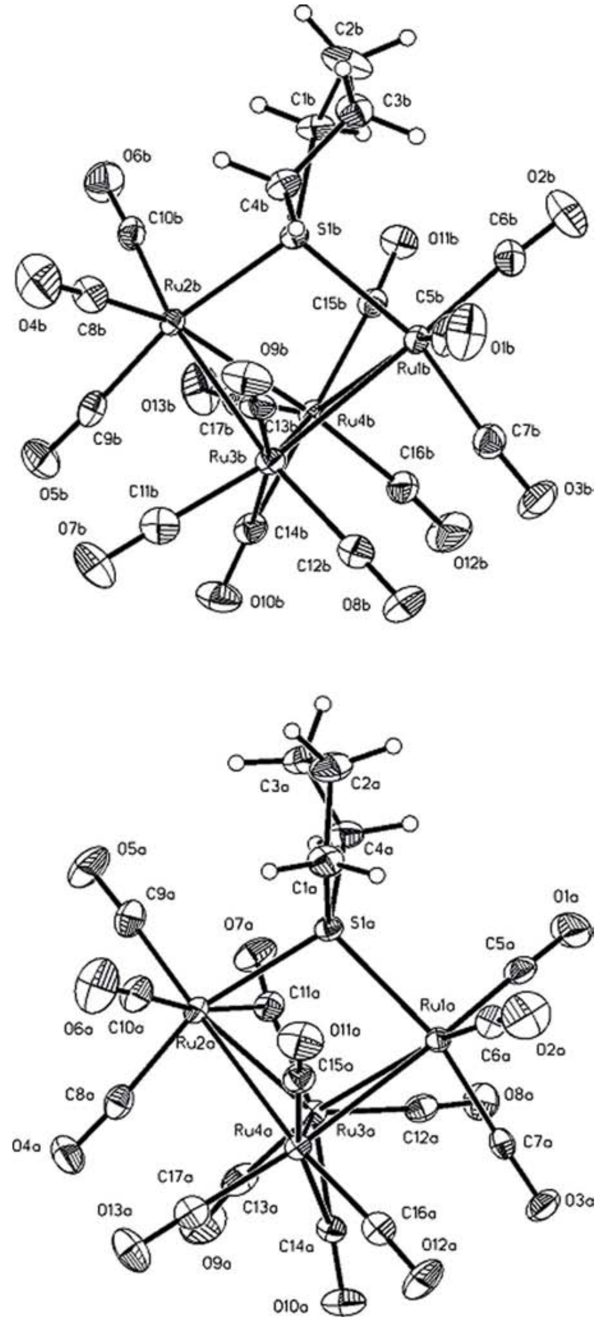

Figure 1. Molecular structures of two isomers of **1a**.

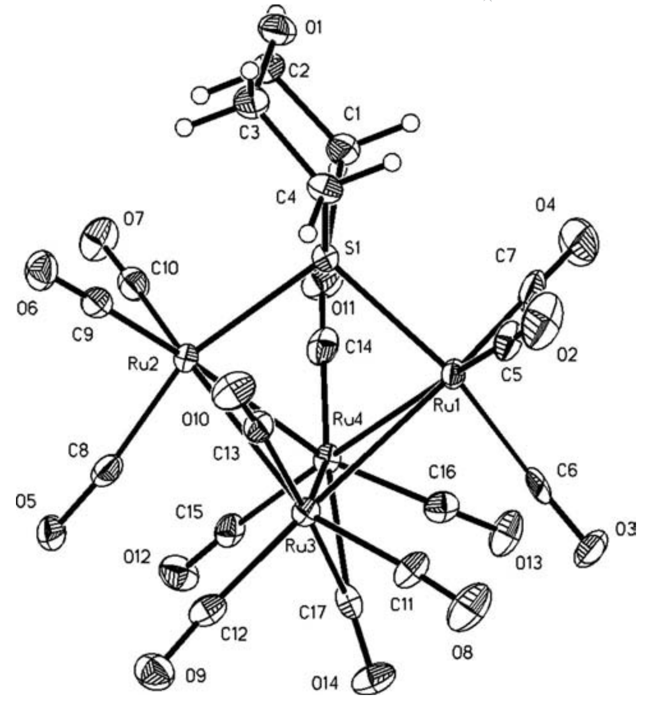

Figure 2. Molecular structure of **1b**.

precipitates of both reactions were transformed into the mononuclear ruthenium complex $[Ru(CO)_3(PPh_3)_2]$ (**2**) by stirring a suspension of the polymer in THF in the presence of an excess amount of triphenylphosphane at room temperature for 6 d. Probably the stronger Lewis base PPh_3 was able to cleave thioether and THF bridges in the polymer. The identity of **2** is shown by a comparison of its experimental data with that already published in the literature.[8]

Scheme 2 shows the photochemical reaction of $[Ru_3(CO)_{12}]$ with the chelating ligand C_2S_2 under reaction conditions already described for the synthesis of **1a** and **1b**. In contrast to the reaction with monodentate thioether ligands, no insoluble precipitate was formed. After chromatographic workup, two ruthenium cluster compounds **3** and **4** were obtained in moderate yields. According to their IR and mass spectra, it became evident that both compounds represent trinuclear ruthenium complexes with one (**3**) and two (**4**) C_2S_2 moieties present in the molecules next to terminal as well as bridging CO ligands. Crystal-structure analyses of both **3** and **4** confirmed that both compounds are most probably produced from $[Ru_3(CO)_{12}]$ just by substitution of two or four CO ligands without any decomposition of the trinuclear cluster core. This is also most probably the reason why no formation of a precipitate was observed in this case. During the formation of tetranuclear compounds **1** from the trinuclear starting material, cluster degradation and aggregation processes must have taken place, therefore also triggering the formation of polynuclear material.

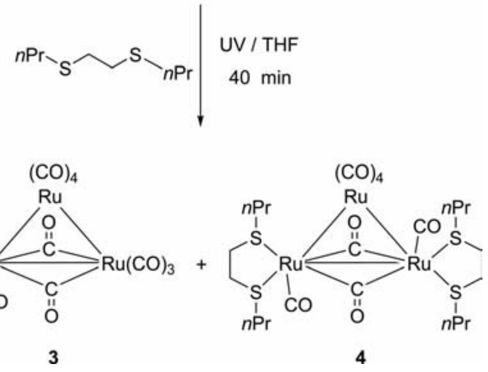

Scheme 2. Photochemical reaction of $[Ru_3(CO)_{12}]$ with chelating C_2S_2 in THF.

Table 1. Bond lengths [pm] and angles [°] of **1a** and **1b**.

Complex **1a** (isomer 1)			
Ru1a–Ru3a	285.75(3)	Ru1a–Ru4a	280.88(3)
Ru2a–Ru3a	281.70(3)	Ru2a–Ru4a	286.84(3)
Ru3a–Ru4a	279.02(3)	Ru1a–S1a	237.95(7)
Ru2a–S1a	239.55(8)	Ru3a–C11a	194.6(3)
Ru2a–C11a	256.3(3)	Ru3a–C14a	201.0(3)
Ru4a–C14a	231.0(3)		
Ru3a–Ru1a–Ru4a	58.992(8)	Ru1a–Ru3a–Ru4a	59.632(8)
Ru1a–Ru4a–Ru3a	61.376(8)	Ru3a–Ru2a–Ru4a	58.774(8)
Ru2a–Ru3a–Ru4a	61.534(8)	Ru2a–Ru4a–Ru3a	59.692(8)
Ru1a–Ru3a–Ru2a	80.161(9)	Ru1a–Ru4a–Ru2a	80.111(9)
Ru1a–S1a–Ru2a	99.93(3)	Ru1a–S1a–C1a	118.7(1)
Ru2a–S1a–C1a	116.2(1)	Ru1a–S1a–C4a	93.1(2)
Ru2a–S1a–C4a	114.0(1)	Ru3a–C11a–O7a	159.0(3)
Ru3a–C14a–O10a	149.4(3)	Ru4a–C14a–O10a	130.3(2)
Complex **1a** (isomer 2)			
Ru1b–Ru3b	286.50(3)	Ru1b–Ru4b	283.16(3)
Ru2b–Ru3b	280.42(3)	Ru2b–Ru4b	284.97(3)
Ru3b–Ru4b	278.54(3)	Ru1b–S1b	237.89(8)
Ru2b–S1b	236.77(7)	Ru4b–C15b	193.2(3)
Ru1b–C15b	266.2(3)	Ru3b–C14b	233.4(3)
Ru4b–C14b	201.4(3)		
Ru3b–Ru1b–Ru4b	58.540(8)	Ru1b–Ru3b–Ru4b	60.131(8)
Ru1b–Ru4b–Ru3b	61.329(8)	Ru3b–Ru2b–Ru4b	59.023(8)
Ru2b–Ru3b–Ru4b	61.304(8)	Ru2b–Ru4b–Ru3b	59.673(8)
Ru1b–Ru3b–Ru2b	80.385(9)	Ru1b–Ru4b–Ru2b	80.185(9)
Ru1b–S1b–Ru2b	100.86(3)	Ru1b–S1b–C1b	115.0(1)
Ru2b–S1b–C1b	117.3(1)	Ru1b–S1b–C4b	114.0(1)
Ru2b–S1b–C4b	119.5(1)	Ru4b–C15b–O11b	162.4(3)
Ru3b–C14b–O10b	129.9(2)	Ru4b–C14b–O10b	150.8(3)
Complex **1b**			
Ru1–Ru3	284.41(6)	Ru1–Ru4	281.66(6)
Ru2–Ru3	285.47(6)	Ru2–Ru4	285.01(6)
Ru3–Ru4	280.31(6)	Ru1–S1	234.7(1)
Ru2–S1	237.2(1)	Ru3–C13	191.7(6)
Ru2–C13	281.7(8)	Ru3–C17	204.1(5)
Ru4–C17	226.9(5)		
Ru3–Ru1–Ru4	59.36(2)	Ru1–Ru3–Ru4	59.83(2)
Ru1–Ru4–Ru3	60.81(2)	Ru3–Ru2–Ru4	58.86(2)
Ru2–Ru3–Ru4	60.49(2)	Ru2–Ru4–Ru3	60.65(2)
Ru1–Ru3–Ru2	79.41(2)	Ru1–Ru4–Ru2	79.95(2)
Ru1–S1–Ru2	101.0(5)	Ru1–S1–C1	113.9(2)
Ru2–S1–C1	117.0(2)	Ru1–S1–C4	114.1(2)
Ru2–S1–C4	117.3(2)	Ru3–C13–O10	167.2(5)
Ru3–C17–O14	148.4(4)	Ru4–C17–O14	130.7(4)

The molecular structure of **3** is depicted in Figure 3; selected bond lengths and angles are summarized in Table 2. Compound **3** consists of a trigonal Ru_3 core in which two ruthenium centers (Ru2, Ru3) are coordinated by three or four terminal CO ligands, respectively. The third Ru atom is coordinated by one CO ligand and C_2S_2 in a chelating fashion. In addition, two bridging CO ligands complete the coordination sphere of Ru1 and Ru2. The three metal–metal bonds are significantly different, with the bond between Ru1 and Ru3 being the longest interaction in the molecule [286.99(7) pm vs. 275.05(8) pm for Ru1–Ru2 and 283.67(8) pm for Ru2–Ru3]. On the other hand, Ru1–Ru2, which is the bond being bridged by two CO ligands, is the shortest metal–metal bond in **3**. One of the bridging CO ligands adopts an almost perfectly symmetrical coordination mode with only small differences in terms of the Ru–C distances. In contrast, the second bridging CO ligand exhibits Ru–C contacts that show a difference of almost 30 pm. Nevertheless, in both ligands the shorter Ru–C bond is always the one towards Ru1 and is in a *trans* position with respect to the coordinating sulfur atoms.

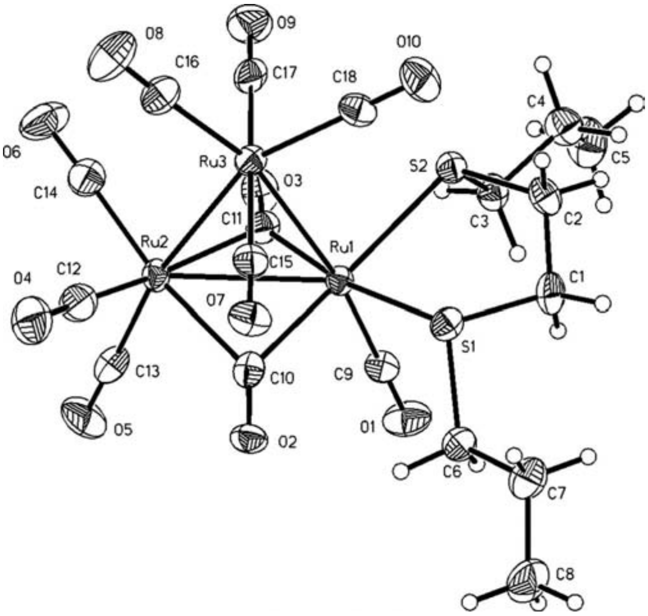

Figure 3. Molecular structure of **3**.

Table 2. Bond lengths [pm] and angles [°] of **3** and **4**.

Complex **3**			
Ru1–Ru2	275.05(8)	Ru1–Ru3	286.99(7)
Ru2–Ru3	283.67(8)	Ru1–S1	243.9(2)
Ru1–S2	244.5(2)	Ru1–C10	205.0(7)
Ru2–C10	211.0(7)	Ru1–C11	197.5(7)
Ru2–C11	226.2(7)		
Ru1–Ru2–Ru3	61.79(2)	Ru2–Ru3–Ru1	57.63(2)
Ru3–Ru1–Ru2	60.58(2)	S1–Ru1–S2	83.94(6)
Ru1–S1–C1	99.1(2)	Ru1–S1–C6	109.5(2)
Ru1–S2–C2	103.7(2)	Ru1–S2–C3	107.5(2)
Complex **4**			
Ru1–Ru1A	268.30(8)	Ru1–Ru2	291.14(6)
Ru1–S1	246.2(1)	Ru1–S2	243.4(1)
Ru1–C9	202.4(6)	Ru1A–C9	204.7(5)
Ru1–Ru2–Ru1A	54.87(2)	Ru2–Ru1–Ru1A	62.56(1)
Ru1–S1–C1	102.7(2)	Ru1–S1–C6	107.8(2)
Ru1–S2–C2	104.1(2)	Ru1–S2–C3	110.6(2)

The molecular structure of **4** is presented in Figure 4; selected bond lengths and angles are also depicted in Table 2. Compound **4** crystallizes in the orthorhombic space group *Pbcn*, with Ru2 being situated on a crystallographic glide plane (*c*). This leads to the fact that the atoms of only one half of the molecule are observed in symmetry-independent positions, whereas the second half of the molecule is created by applying the corresponding symmetry operation. This also leads to the crystallographically observed *syn* arrangement of the C_2S_2 ligands. NMR spectra show only one set of signals for C_2S_2 as well as for CO ligands. This suggests that an average spectrum of highly fluxional *syn* and *anti* isomers is observed. Both chelating ligands are coordinated at the ruthenium centers, which are bridged by two carbonyl ligands. Again the respective Ru1–Ru1A bond is significantly shorter than the other metal–metal bonds. Due to crystallographic symmetry in **4**, both bridging CO ligands show an identical coordination mode with only slight differences in the Ru–C bond lengths.

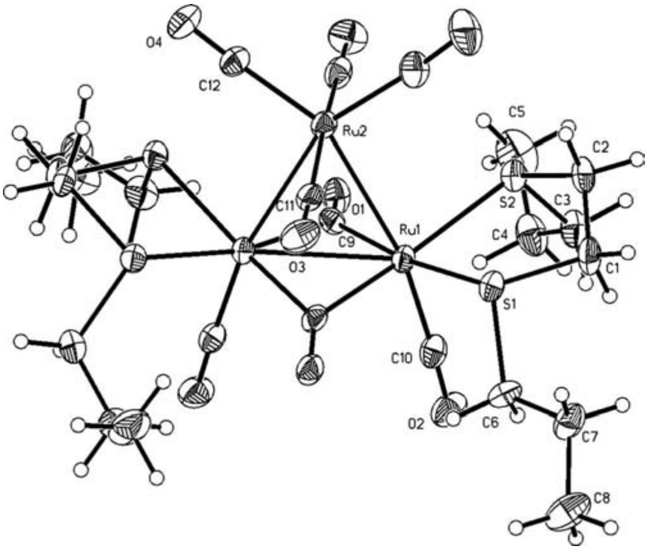

Figure 4. Molecular structure of **4**.

To the best of our knowledge the only highly related compounds that were structurally characterized were derived from [$Ru_3(CO)_{12}$] by substituting three terminal CO ligands at one ruthenium atom with tridentate thioether ligands (1,4,7-trithianonane and 1,5,9-trithiadodecane).[9]

In a previous report on the photochemical reaction of [$Ru_3(CO)_{12}$] with thioether ligands in $CHCl_3$, we observed the formation of mono- and dinuclear Ru^{II} complexes that contained chlorido ligands. The latter obviously originated from the chlorinated solvent.[6] We therefore concluded that in a first step thioether ligands substituted CO ligands that were labilized by irradiation, and in a subsequent reaction step the oxidative cleavage of the trinuclear ruthenium cluster core took place. We therefore dissolved compound **4**, which corresponds to the proposed intermediates in chlorinated solvents, and analyzed the reaction products (Scheme 3).

Under inert conditions, the trinuclear ruthenium compound **4** upon being dissolved in chloroform or dichloromethane yielded the mononuclear ruthenium(II) complex **5**. The reaction in CH_2Cl_2 proceeded considerably slower. Compound **5** has been isolated from the photochemically induced reaction of [$Ru_3(CO)_{12}$] with C_2S_2 in $CHCl_3$ before, and its spectroscopic and structural features have been described in a previous report.[6] Nevertheless, if **4** is dissolved in chloroform in the presence of oxygen, the dinuclear chlorido-bridged complex **6** is produced in good yields. The same compound may be obtained from **5** if a solution is allowed to stand under air for another 2 d. Most probably the reaction that starts from **4** also proceeds via intermediate **5**, although much faster than the situation without atmospheric oxygen being present. Dimerization then occurs after the loss of one CO ligand from **5** to produce **6**.

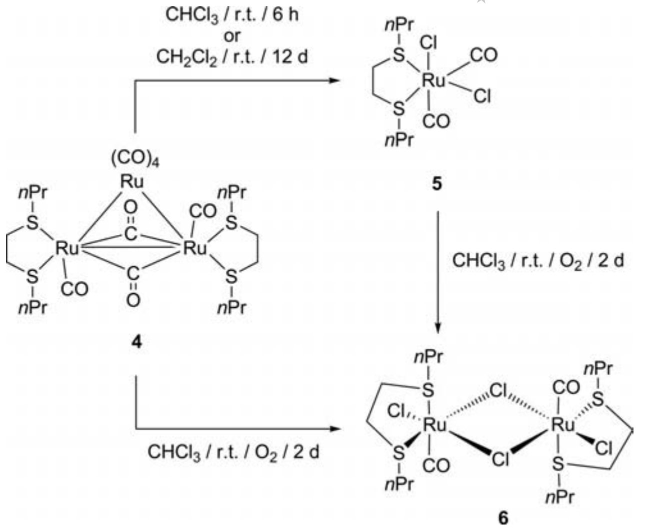

Scheme 3. Oxidative cleavage of the Ru_3 cluster core by the reaction of **4** with chlorinated solvents.

The molecular structure of **6** is presented in Figure 5; selected bond lengths and angles are summarized in Table 3. The center of the Ru_2Cl_2 ring represents a crystallographic center of inversion that leads to an *anti* orientation of the two C_2S_2 ligands. ^{13}C NMR spectra also showed only one set of resonances with regards to the C_2S_2 moieties. In the molecular structure of **6**, both Ru^{II} centers are octahedrally coordinated by the chelating bis(thioether) C_2S_2, one CO ligand, and one terminal and two bridging

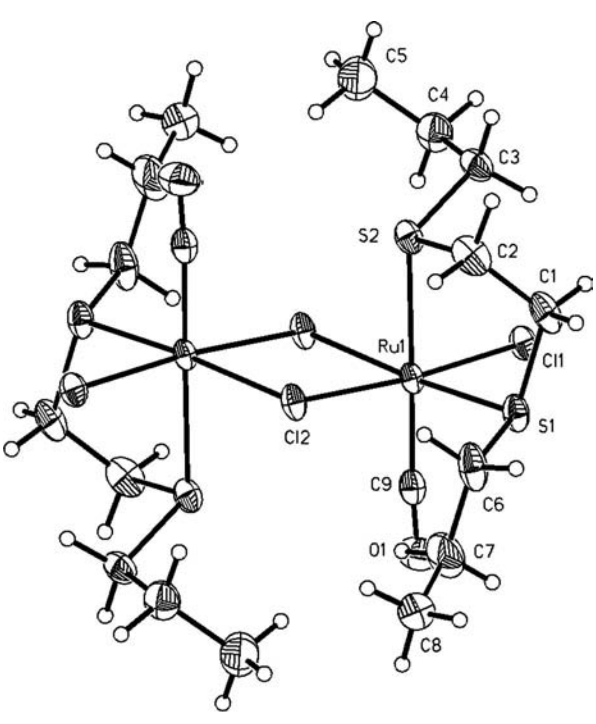

Figure 5. Molecular structure of **6**.

chlorido ligands. As expected, Ru–Cl bonds in the central four-membered ring are longer than the bond towards the terminal chlorido ligands. Also, ruthenium–sulfur bonds differ significantly due to the different *trans* effects of carbon monoxide and the bridging chlorido ligand.

Table 3. Bond lengths [pm] and angles [°] of **6**.

Ru1–Cl1	239.3(2)	Ru1–Cl2	241.5(2)
Ru1–Cl2A	244.8(2)	Ru1–S1	231.0(2)
Ru1–S2	245.4(2)	Ru1–C9	185.6(8)
Cl1–Ru1–Cl2	174.97(6)	Cl1–Ru1–Cl2A	92.84(6)
Cl1–Ru1–S1	86.31(6)	Cl1–Ru1–S2	93.28(6)
Cl1–Ru1–C9	89.4(2)	Cl2–Ru1–Cl2A	83.52(6)
Cl2–Ru1–S1	97.09(6)	Cl2–Ru1–S2	83.16(6)
Cl2–Ru1–C9	94.2(2)	Cl2A–Ru1–S1	175.98(7)
Cl2A–Ru1–S2	88.06(6)	Cl2A–Ru1–C9	93.7(2)
S1–Ru1–S2	88.07(6)	S1–Ru1–C9	90.3(2)
S2–Ru1–C9	176.7(2)		

To the best of our knowledge, **6** is the first structurally characterized halido-bridged Ru^{II} complex with thioether ligands. All related compounds for which structural data are available exhibit either mono- or bidentate phosphane ligands or, in one case, diphosphaferrocene as a chelating ligand.[10]

Conclusion

The photochemically induced reaction of [Ru$_3$(CO)$_{12}$] with monodentate and bidentate thioether ligands in THF leads to the formation of ruthenium–carbonyl cluster compounds with the respective thioether ligands. In the case of monodentate thioethers, tetranuclear compound **1** is observed in low yields next to polymeric material. If bidentate ligands are used, trinuclear substitution products **3** and **4** with one and two bis(thioether) ligands are observed. The latter may be oxidatively cleaved upon reaction with chlorinated solvents under inert conditions or under atmospheric oxygen. This reaction allows the isolation of the first structurally characterized halido-bridged dinuclear Ru^{II} complex with thioether ligands **6**. This compound may serve as the starting compound to mononuclear ruthenium compounds of the general formula [Ru(CO)Cl$_2$(RS∩SR)L] after cleaving chlorido bridges with additional Lewis basic ligands L. In addition, the reaction of **4** to mononuclear compounds **5** sheds some light on highly related photochemical reactions in CHCl$_3$ as solvent in which compounds of this type are the main products. With respect to the results described herein, it is highly reasonable that the reaction in CHCl$_3$ initially also produces substitution products of type **4**, which are then converted in situ into complexes of type **5**.

Experimental Section

General: All procedures were carried out under argon in anhydrous, freshly distilled solvents. [Ru$_3$(CO)$_{12}$] was purchased from ABCR; 1,4-oxathiane and tetrahydrothiophene were purchased from Aldrich and used without further purification. 1-[2-(Propylsulfanyl)-ethylsulfanyl]propane was synthesized according to a modified literature procedure, and its identity was shown by comparison of NMR spectra.[11] Solvents were dried and distilled before use.[12] Photochemical reactions were performed in a water-cooled 150 mL photoreactor with UV light irradiation of 150 W. IR spectra were performed in a range of 400–4000 cm^{-1} by using KBr pellets with a Perkin–Elmer System 2000 device. Mass spectra were obtained with a Finnigan MAT SSQ 710 device. NMR spectra were recorded with a Bruker DRX 400 spectrometer (^{1}H: 400.13 MHz; ^{13}C: 100.62 MHz; solvent as internal standard). Elemental analyses were performed at the Institute of Organic Chemistry and Macromolecular Chemistry, Friedrich Schiller University Jena.

X-ray Structure Determinations: Intensity data were collected with a Nonius Kappa CCD diffractometer by using graphite-monochromated Mo-K_α radiation. Data were corrected for Lorentz polarization but not for absorption effects.[13,14] Crystallographic data as well as structure-solution and refinement details are summarized in Table 4. Structures were solved by direct methods (SHELXS) and refined by full-matrix least-squares techniques against $F_o{}^2$ (SHELXL-97).[15,16] Hydrogen atoms were included at calculated positions with fixed thermal parameters. All non-hydrogen, non-disordered atoms were refined anisotropically.[16] XP (SIEMENS Analytical X-ray Instruments, Inc.) was used for structure representations. CCDC-776990 (**1a**), -776991 (**1b**), -776992 (**3**), -776993 (**4**), and -776994 (**6**) contain the supplementary crystallographic data for this paper. These data can be obtained free of charge from The Cambridge Crystallographic Data Centre via www.ccdc.cam.ac.uk/data_request/cif.

Synthesis and Analytical Data of 1a and 1b: [Ru$_3$(CO)$_{12}$] (105 mg, 0.16 mmol) and the corresponding thioether ligand (THT: 176 mg, 2 mmol; OXT: 208 mg, 2 mmol) were dissolved in anhydrous tetrahydrofuran (THF; 120 mL), and the resulting solution was stirred and irradiated with UV light. Within 10 min, an orange precipitate started to form. The reaction mixture was irradiated for 40 min. The precipitate was collected by filtration and washed twice with THF, thereby resulting in an orange solid (35 mg). The remaining solution was concentrated to dryness, and the product mixture was subjected to column chromatography on silica. By using light petroleum (b.p. 40–60 °C) as the eluent, a yellow band was obtained that was identified as [Ru$_3$(CO)$_{12}$] (THT: 40 mg, OXT: 46 mg). A second red band was collected by using light petroleum/THF (10:1) as eluent. Yield **1a**: 6 mg (9% based on reacted [Ru$_3$(CO)$_{12}$]); **1b**: 4 mg (6%). Crude **1a** or **1b** may be recrystallized from a concentrated solution in THF/light petroleum at 0 °C to produce single crystals suitable for X-ray diffraction.

Compound 1a: ^{1}H NMR ([D$_8$]THF, 298 K): δ = 2.44 (br., 4 H, CH$_2$), 3.71 (br., 4 H, SCH$_2$) ppm. IR (KBr): $\tilde{\nu}$ = 1613, 1873, 1983, 2024, 2081 (CO), 2963 (C–H of THT) cm^{-1}. MS (FAB, nitrobenzyl alcohol): *m*/*z* = 857 [M + H]$^+$, 829 [M + H – CO]$^+$, 801 [M + H – 2 CO]$^+$, 773 [M + H – 3 CO]$^+$, 745 [M + H – 4 CO]$^+$, 717 [M + H – 5 CO]$^+$, 688 [M – 6 CO]$^+$, 660 [M – 7 CO]$^+$, 632 [M – 8 CO]$^+$, 604 [M – 9 CO]$^+$. C$_{17}$H$_8$O$_{13}$Ru$_4$S$_1$ (856.58): calcd. C 23.83, H 0.93, S 3.74; found C 25.08, H 1.27, S 2.92.

Analytical Data of the Precipitate: Found C 18.50, H 0.69, S 0.55. IR (KBr): $\tilde{\nu}$ = 511, 591, 822. 1102, 1263, 1512, 1603, 2037, 2960, 3436 cm^{-1}.

Compound 1b: ^{1}H NMR ([D$_8$]THF, 298 K): δ = 2.65–2.82 (m, 4 H, SCH$_2$), 4.18–4.34 (m, 4 H, OCH$_2$) ppm. IR (KBr): $\tilde{\nu}$ = 1619, 1884, 1986, 2033, 2083 (CO), 2963 (C–H of OXT) cm^{-1}. MS (FAB, nitrobenzyl alcohol): *m*/*z* = 872 [M]$^+$, 844 [M – CO]$^+$, 816 [M – 2 CO]$^+$, 788 [M – 3 CO]$^+$, 760 [M – 4 CO]$^+$, 732 [M – 5 CO]$^+$, 704 [M – 6 CO]$^+$, 676 [M – 7 CO]$^+$, 648 [M – 8 CO]$^+$, 620 [M – 9 CO]$^+$, 463 [Ru(CO)$_2$(OXT)]$^+$, 398 [Ru$_2$(CO)$_7$]$^+$, 341 [Ru$_2$(CO)$_5$]$^+$.

Table 4. Crystal data and refinement details for the X-ray structure determinations of **1a**, **1b**, **3**, **4**, and **6**.

	1a	**1b**	**3**	**4**	**6**
Empirical formula	$C_{17}H_8O_{13}Ru_4S$	$C_{17}H_8O_{14}Ru_4S$	$C_{18}H_{18}O_{10}Ru_3S_2$	$C_{24}H_{36}O_8Ru_3S_4$	$C_{18}H_{36}Cl_4O_2Ru_2S_4\cdot 2CHCl_3$
M_r [g mol^{-1}]	856.57	872.57	761.65	883.98	995.38
T [°C]	–90(2)	–140(2)	–90(2)	–90(2)	–140(2)
Crystal system	monoclinic	monoclinic	monoclinic	orthorhombic	monoclinic
Space group	$C2/c$	$P2_1/c$	Cc	$Pbcn$	$P2_1/c$
a [Å]	28.6136(6)	9.3671(5)	19.5255(11)	14.2198(8)	12.5166(6)
b [Å]	16.9148(3)	14.8469(7)	11.4502(8)	15.8002(8)	7.4571(3)
c [Å]	19.3762(2)	17.1782(7)	14.5467(6)	14.3596(7)	20.6840(9)
α [°]	90	90	90	90	90
β [°]	92.505(1)	96.574(3)	127.680(3)	90	102.750(3)
γ [°]	90	90	90	90	90
V [Å^3]	9369.0(3)	2373.31(19)	2573.9(3)	3226.3(3)	1882.99(15)
Z	16	4	4	4	2
ρ [g cm^{-3}]	2.429	2.442	1.965	1.820	1.756
μ [cm^{-1}]	26.84	26.54	19.47	16.87	17.53
Measured data	32772	16495	8692	20469	12211
Data with $I > 2\sigma(I)$	9047	3613	4150	2075	2774
Unique data/R_{int}	10711/0.0328	5429/0.0814	5000/0.0465	3688/0.1371	4307/0.0769
wR_2 (all data, on F^2)[a]	0.0564	0.0770	0.0730	0.0888	0.1743
R_1 [$I > 2\sigma(I)$][a]	0.0253	0.0403	0.0367	0.0427	0.0623
s[b]	1.021	0.952	0.970	0.925	1.012
Residual density [e Å^{-3}]	0.599/–0.948	0.875/–0.877	0.575/–0.870	0.621/–0.756	2.569/–1.280
Flack parameter	–	–	–0.10(4)	–	–

[a] Definition of the R indices: $R_1 = (\Sigma||F_o| - |F_c||)/\Sigma|F_o|$; $wR_2 = \{\Sigma[w(F_o^2 - F_c^2)^2]/\Sigma[w(F_o^2)^2]\}^{1/2}$ with $w^{-1} = \sigma^2(F_o^2) + (aP)^2 + bP$; $P = [2F_c^2 + \max(F_o^2)]/3$. [b] $s = \{\Sigma[w(F_o^2 - F_c^2)^2]/(N_o - N_p)\}^{1/2}$.

$C_{17}H_8O_{14}Ru_4S_1$ (872.58): calcd. C 23.39, H 0.91, S 3.65; found C 23.98, H 1.15, S 3.01.

Analytical Data of the Precipitate: Found C 19.77, H 0.71, S 0.59. IR (KBr): ṽ = 513, 591, 821. 1109, 1263, 1513, 1612, 1976, 2040, 2960, 2963, 3429 cm^{-1}.

When the insoluble precipitate (15 mg) that is formed during the photochemical reaction of $[Ru_3(CO)_{12}]$ and THT or OXT was suspended in THF (5 mL) and stirred at room temperature in the presence of PPh_3 (100 mg) for 6 d, the precipitate fully dissolved, thereby resulting in an orange solution. After evaporation of the solvent and washing of the orange residue with light petroleum (b.p. 40–60 °C) (3×), **2** was obtained as an yellow-orange solid. Crystallization was achieved by diffusion of light petroleum into a concentrated solution of **2** in THF at room temperature. Yield **2**: 20 mg. MS and X-ray data correspond to results already published.[8]

Synthesis and Analytical Data of 3 and 4: $[Ru_3(CO)_{12}]$ (105 mg, 0.16 mmol) was dissolved in THF together with C_2S_2 (2 mmol, 355 mg), and the solution was stirred and irradiated with UV light. After 40 min, the solution was still clear, and, after evaporation of the solvent, an orange-red oily residue formed. Chromatographic workup of the crude reaction mixture first yielded $[Ru_3(CO)_{12}]$ (30 mg) by using light petroleum (b.p. 40–60 °C). With a mixture of light petroleum/THF (10:1), **4** was eluted as a pink solution. Encrease of the polarity of the eluent to light petroleum/THF (5:1) led to the isolation of **3** as a red band. Yields: **3** {30 mg, 33% calcd. on reacted $[Ru_3(CO)_{12}]$}, **4** (15 mg, 15%). In another experiment, $[Ru_3(CO)_{12}]$ (0.63 mmol, 400 mg) was irradiated together with C_2S_2 (7.58 mmol, 1.352 g) for 120 min. After chromatographic workup, **4** {149 mg, 30% based on reacted $[Ru_3(CO)_{12}]$} and **3** (79 mg, 18%) were observed. Crystallization for **3** and **4** was possible by diffusion of light petroleum into a concentrated solution of the respective compound in THF at room temperature.

Compound 3:. ^{1}H NMR ([D$_8$]THF, 298 K): δ = 1.09 (t, $^3J_{H,H}$ = 7.2 Hz, 6 H, CH_3), 1.83 (br., 4 H, CH_2), 2.86 (br., 4 H, CH_2), 3.07 (br., 4 H, CH_2) ppm. ^{13}C NMR ([D$_8$]THF, 298 K): δ = 13.2 (CH_3), 23.2 (CH_2), 35.9 (SCH_2), 44.3 (SCH_2), 207.8 (CO) ppm. IR (KBr): ṽ = 1741, 1979, 2029, 2076 (CO), 2876, 2934, 2967 (C–H of C_2S_2) cm^{-1}. MS (FAB, nitrobenzyl alcohol): m/z = 761 [M]$^+$, 733 [M – CO]$^+$, 718 [M–CO–Me]$^+$, 705 [M – 2 CO]$^+$, 690 [M – 2 CO – Me]$^+$, 677 [M – 3 CO]$^+$, 662 [M – 3 CO – Me]$^+$, 649 [M – 4 CO]$^+$, 634 [M – 4 CO – Me]$^+$, 621 [M – 5 CO]$^+$, 606 [M – 5 CO – Me]$^+$, 593 [M – 6 CO]$^+$, 578 [M – 6 CO – Me]$^+$, 565 [M – 7 CO]$^+$, 550 [M – 7 CO – Me]$^+$, 537 [M – 8 CO]$^+$, 522 [M – 8 CO – Me]$^+$, 509 [M – 9 CO]$^+$, 494 [M – 9 CO – Me]$^+$, 481 [M – 10 CO]$^+$, 466 [M – 10 CO – Me]$^+$, 451 [M – 10 CO – 2 Me]$^+$, 437 [M – 10 CO – 2 Me – CH_2]$^+$, 423 [M – 10 CO – 2 Me – 2 CH_2]$^+$, 409 [M – 10 CO – 2 Me – 3 CH_2]$^+$. $C_{18}H_{18}O_{10}Ru_3S_2$ (761.67): calcd. C 28.38, H 2.37, S 8.41; found C 28.92, H 2.48, S 8.57.

Compound 4: ^{1}H NMR ([D$_8$]THF, 298 K): δ = 1.12 (t, $^3J_{H,H}$ = 7.2 Hz, 6 H, CH_3), 1.81–1.95 (m, 4 H, CH_2), 2.79–2.93 (m, 4 H, CH_2), 3.05–3.19 (m, 4 H, CH_2) ppm. ^{13}C NMR ([D$_8$]THF, 298 K): δ = 13.5 (CH_3), 23.5 (CH_2), 36.1 (SCH_2), 44.5 (SCH_2), 207.7 (CO) ppm. IR (KBr): ṽ = 1763, 1948, 2029 (CO), 2875, 2933, 2966 (C–H of C_2S_2) cm^{-1}. MS (FAB, nitrobenzyl alcohol): m/z = 883 [M]$^+$, 855 [M – CO]$^+$, 827 [M – 2 CO]$^+$, 799 [M – 3 CO]$^+$, 784 [M – 3 CO – Me]$^+$, 771 [M – 4 CO]$^+$, 756 [M – 4 CO – Me]$^+$, 743 [M – 5 CO]$^+$, 728 [M – 5 CO – Me]$^+$, 715 [M – 6 CO]$^+$, 700 [M – 6 CO – Me]$^+$, 687 [M – 7 CO]$^+$, 672 [M – 7 CO – Me]$^+$, 659 [M – 8 CO]$^+$, 644 [M – 8 CO – Me]$^+$, 629 [M – 8 CO – 2 Me]$^+$, 615 [M – 8 CO – 2 Me – CH_2]$^+$, 601 [M – 8 CO – 2 Me – 2 CH_2]$^+$, 587 [M – 8 CO – 2 Me – 3 CH_2]$^+$, 573 [M – 8 CO – 2 Me – 4 CH_2]$^+$, 473 [$Ru_3S_4C_2H_5$]$^+$. $C_{24}H_{36}O_8Ru_3S_4$ (883.99): calcd. C 32.62, H 4.07, S 14.50; found C 32.83, H 4.38, S 13.88.

Synthesis and Analytical Data of 5 and 6: A sample of **4** (0.017 mmol, 15 mg) was dissolved in anhydrous $CHCl_3$ (10 mL), and the solution was kept under inert conditions at room temperature for 6 h. The color of the solution changed from pink to yellow. After evaporation of the solvent, the residue was washed with light petroleum (b.p. 40–60 °C) to give an orange solution that contained $[Ru_3(CO)_{12}]$ (3 mg, 27.6%). The remaining residue might be recrystallized by diffusion of light petroleum into a solution in $CHCl_3$ to yield **5** (9 mg, 43%). The identity of **5** was demonstrated by comparison of analytical data with the compound produced from photolysis of $[Ru_3(CO)_{12}]$ in $CHCl_3$ in the presence of C_2S_2.[6] When the above-mentioned solution of **5** was exposed to air, orange block-shaped crystals of **6** were produced after 2 d of standing at room temperature. Yield 8 mg (62%).

Compound 6: $C_{18}H_{36}Cl_4O_2Ru_2S_4$ (756.67): calcd. C 28.57, H 4.76, S 16.93; found C 28.92, H 4.86, S 16.55. IR (KBr): $\tilde{\nu}$ = 1967 (br., CO), 2873, 2929, 2965 (C–H of C_2S_2) cm^{-1}. ^1H NMR (CD_2Cl_2, 298 K): δ = 1.01 (dt, $^3J_{H,H}$ = 7.2 Hz, $^4J_{H,H}$ = 2.4 Hz, 6 H, CH_3), 1.22 (dt, $^3J_{H,H}$ = 7.2 Hz, $^4J_{H,H}$ = 2.4 Hz, 6 H, CH_3), 1.50–1.69 (m, 4 H, CH_2), 1.89–2.08 (m, 4 H, CH_2), 2.11–3.35 (m, 16 H, CH_2) ppm. ^{13}C NMR (in CD_2Cl_2, 298 K): δ = 13.2 (br., CH_3), 14.1 (CH_3), 22.7 (CH_2), 29.4 (CH_2), 31.9 (CH_2) ppm. MS (FAB, nitrobenzyl alcohol): m/z = 757 $[M]^+$, 729 $[MH - CO]^+$, 614 $[M - 2 CO - 2 Cl - Me]^+$.

Acknowledgments

Financial support by the Thüringer Aufbaubank is gratefully acknowledged.

[1] N. N. Greenwood, A. Earnshaw, *Chemistry of the Elements*, VCH, Weinheim, **1988**.

[2] For recent reviews, see: a) H. Rang, J. Kann, V. Oja, *Oil Shale* **2006**, *23*, 164–176; b) R. A. Pandey, S. Malhotra, *Crit. Rev. Env. Sci. Technol.* **1999**, *29*, 229–268; c) D. J. Monticello, *CHEMTECH* **1998**, *28*, 38–45.

[3] a) C. Gandolfi, M. Heckenroth, A. Neels, G. Laurenczy, M. Albrecht, *Organometallics* **2009**, *28*, 5112–5121; b) Y. Ohki, Y. Takikawa, H. Sadohara, C. Kesenheimer, B. Engendahl, E. Kapatina, K. Tatsumi, *Chem. Asian J.* **2008**, *3*, 1625–1635; c) A. Ben-Asuly, E. Tzur, C. E. Diesendruck, M. Sigalov, I. Goldberg, N. G. Lemcoff, *Organometallics* **2008**, *27*, 811–813; d) S. Takemoto, H. Kawamura, Y. Yamada, T. Okada, A. Ono, E. Yoshikawa, Y. Mizobe, M. Hidai, *Organometallics* **2002**, *21*, 3897–3904; e) T. Okumura, Y. Morishima, H. Shiozaki, T. Yagju, Y. Funahashi, T. Ozawa, K. Jitsukawa, H. Masuda, *Bull. Chem. Soc. Jpn.* **2007**, *80*, 507–517; f) D. P. Riley, *Inorg. Chim. Acta* **1985**, *99*, 5–11; g) D. P. Riley, J. D. Oliver, *Inorg. Chem.* **1986**, *25*, 1814–1821; h) D. P. Riley, J. D. Oliver, *Inorg. Chem.* **1986**, *25*, 1821–1825; i) D. P. Riley, J. D. Oliver, *Inorg. Chem.* **1986**, *25*, 1825–1830; j) D. P. Riley, M. R. Thompson, J. Lyon III, *J. Coord. Chem.* **1989**, *19*, 49–59.

[4] a) E. Bouwman, W. L. Driessen, J. Reedijk, *Coord. Chem. Rev.* **1990**, *104*, 143–172; b) J.-R. Li, X.-H. Bu, *Eur. J. Inorg. Chem.* **2008**, 27–40; c) M. Brorson, J. D. King, K. Kiriakidou, F. Prestopino, E. Nordlander, in *Metal Clusters in Chemistry*, vol. 2 (Eds.: P. Braunstein, L. A. Oro, P. R. Raithby), Wiley-VCH, Weinheim, **1999**, pp. 741–781.

[5] a) R. D. Adams, *J. Cluster Sci.* **1992**, *3*, 263–273; b) H. Li, G. B. Carpenter, D. A. Sweigart, *Organometallics* **2000**, *19*, 1823–1825; c) J. G. Planas, M. Hirano, S. Komiya, *Chem. Commun.* **1999**, 1793–1794; d) D. A. Vicic, W. D. Jones, *J. Am. Chem. Soc.* **1999**, *121*, 7606–7617; e) C. A. Dullaghan, X. Zhang, D. L. Greene, G. B. Carpenter, D. A. Sweigart, C. Camiletti, E. Rajaseelan, *Organometallics* **1998**, *17*, 3316–3322; f) A. W. Myers, W. D. Jones, *Organometallics* **1996**, *15*, 2905–2917; g) J. H. Yamamoto, G. P. A. Yap, C. M. Jensen, *J. Am. Chem. Soc.* **1991**, *113*, 5060–5061.

[6] B. Maiti, H. Görls, O. Klobes, W. Imhof, *Dalton Trans.* **2010**, *39*, 5713–5720.

[7] a) S. Rossi, J. Pursiainen, T. A. Pakkanen, *J. Organomet. Chem.* **1992**, *436*, 55–71; b) R. D. Adams, J. A. Belinski, *J. Cluster Sci.* **1990**, *1*, 319–333; c) S. Rossi, J. Pursiainen, T. A. Pakkanen, *Organometallics* **1991**, *10*, 1390–1394; d) T. Teppana, S. Jaaskelainen, M. Ahlgren, J. Pursiainen, T. A. Pakkanen, *J. Organomet. Chem.* **1995**, *486*, 217–228.

[8] F. Dahan, S. Rabo, B. Chaudret, *Acta Crystallogr., Sect. C* **1984**, *40*, 786–788.

[9] R. D. Adams, J. H. Yamamoto, *Organometallics* **1995**, *14*, 3704–3711.

[10] a) A. V. Marchenke, J. C. Huffman, P. Valerga, M. J. Tenorio, M. C. Puerta, K. G. Caulton, *Inorg. Chem.* **2001**, *40*, 6444–6450; b) G. Espino, F. A. Jalón, M. Maestro, B. R. Manzano, M. Pérez-Manrique, A. C. Bacigalupe, *Eur. J. Inorg. Chem.* **2004**, 2542–2552; c) B. Deschamps, F. Mathey, J. Fischer, J. H. Nelson, *Inorg. Chem.* **1984**, *23*, 3455–3462; d) V. Cadierno, P. Crochet, J. Díez, S. E. García-Garrido, J. Gimeno, S. García-Granda, *Organometallics* **2003**, *22*, 5226–5234; e) S. D. Drouin, S. Monfette, D. Amoroso, G. P. A. Yap, D. E. Fogg, *Organometallics* **2005**, *24*, 4721–4728; f) E. Mothes, S. Sentets, M. A. Luquin, R. Mathieu, N. Lugan, G. Lavigne, *Organometallics* **2008**, *27*, 1193–1206; g) T. G. Southern, P. H. Dixneuf, J. Y. Le Marouille, D. Grandjean, *Inorg. Chem.* **1979**, *18*, 2987–2991.

[11] N. V. Russavskaya, N. A. Korchevin, O. V. Alekminskaya, E. N. Sukhomazova, E. P. Levanova, E. N. Deryagina, *Russ. J. Org. Chem.* **2002**, *38*, 1445–1448.

[12] D. D. Perrin, W. L. F. Armarego, D. R. Perrin, *Purification of Laboratory Chemicals*, Pergamon Press, New York, **1980**.

[13] *COLLECT*, Data Collection Software, B. V. Nonius , Netherlands, **1998**.

[14] Z. Otwinowski, W. Minor, *Processing of X-ray Diffraction Data Collected in Oscillation Mode* in *Methods in Enzymology* (Eds.: C. W. Carter, R. M. Sweet), Academic Press, **1997**, vol. 276 (“Macromolecular Crystallography”), part A, pp. 307–326.

[15] G. M. Sheldrick, *Acta Crystallogr., Sect. A* **1990**, *46*, 467–473.

[16] G. M. Sheldrick, *Acta Crystallogr., Sect. A* **2008**, *64*, 112–122.

Received: August 10, 2010